Available online at www.sciencedirect.com
SCIENCE DIRECT®
Journal of Magnetic Resonance 169 (2004) 246–249
JMR Journal of Magnetic Resonance
www.elsevier.com/locate/jmr

meta-DENSE complex acquisition for reduced intravoxel dephasing

Anthony H. Aletras* and Andrew E. Arai

Laboratory of Cardiac Energetics, US Department of Health and Human Services, National Heart, Lung and Blood Institute, National Institutes of Heath, Bethesda, MD, USA

Received 19 December 2003; revised 5 May 2004
Available online 7 June 2004

Abstract

Displacement encoding with stimulated echoes (DENSE) with a meta-DENSE readout and RF phase cycling to suppress the STEAM anti-echo is described for reducing intravoxel dephasing signal loss. This RF phase cycling scheme, when combined with existing meta-DENSE suppression of the T_1 recovering signal, yields higher quality DENSE myocardial strain maps. Phantom and human images are provided to demonstrate the technique, which is capable of acquiring phase contrast displacement encoded images at low encoding gradient strengths providing better spatial resolution and less signal loss due to intravoxel dephasing than prior methods.
Published by Elsevier Inc.

Keywords: Myocardial; Contraction; Cardiac; Function; SPAMM; DENSE; HARP; Tagging; Heart; MRI

1. Introduction

STEAM [1] has been used for phase contrast imaging of myocardial displacement and strain with displacement encoding with stimulated echoes (DENSE) [2–5]. The acquisition of displacement maps has been accomplished by suppressing the T_1-recovering signal (FID or DC) [4–7], which is a potential source of image quality degradation. For a given displacement encoding strength, this allowed larger k-space areas to be sampled by reducing the interference of the desired displacement encoded stimulated echo and this non-encoded T_1-recovering signal [8]. However, STEAM experiments result in 50% signal loss [9] due to the inability to store both real and imaginary components of the position encoded magnetization along the longitudinal axis thus giving rise to the complex conjugate of the desired signal, i.e., the stimulated anti-echo [10]. For a given displacement encoding strength, the anti-echo can also create tag-like artifacts if large enough areas of k-space are sampled for even higher spatial resolution DENSE images. Increasing the gradient encoding strength to shift the anti-echo outside the sampled k-space window results in signal loss from intravoxel dephasing [11] thus negating the benefits of a smaller pixel size.

The acquisition of both the real and imaginary components of the magnetization in successive acquisitions and summing them to yield the whole position encoded complex signal, which does not contain the anti-echo, has been shown [12]. Phantom as well as human images and myocardial strain maps with a meta-DENSE readout [4] are shown using this RF phase cycling scheme. Compared to prior meta-DENSE implementations, images of improved quality can be acquired by using inversion recovery and RF-cycling so as to reduce intravoxel dephasing related signal loss.

2. Methods

All experiments were performed with a General Electric Medical Systems (Waukesha, WI) 1.5 T cardiovascular magnet. Phantom data were acquired with the standard cardiac four coil phased array. The phantom consisted of a $CuSO_4$ doped saline container (T_1 825 ms) to simulate the myocardium. Imaging parameters similar

* Corresponding author. Fax: 1-301-402-2389.
E-mail address: AletrasA@nhlbi.nih.gov (A.H. Aletras).

1090-7807/$ - see front matter. Published by Elsevier Inc.
doi:10.1016/j.jmr.2004.05.008

to those used for the human experiments, as described below, were used.

DENSE images were acquired from a human normal volunteer. Position encoding was performed as described previously [2–4] following the detection of the QRS complex at 1.2, 2.0, and 4.0 mm/π. Note that, since it requires a higher gradient encoding moment, 1.2 mm/π corresponds to a stronger encoding strength than 4.0 mm/π. Displacement encoded images were acquired at end systole (encoding interval of approximately 300 ms) with meta-DENSE [4] and an echo train length of 32 at ±62.5 kHz. The matrix size was 128×96 thus resulting in a 158 ms/heartbeat readout. With two dummy scans to set up steady-state and two RF cycled acquisitions, the total acquisition time was 20 heartbeats since X-encoded, Y-encoded and a reference scan were acquired. The voxel size was $2.8 \times 2.8 \times 7\,\text{mm}^3$. Images were also acquired at higher spatial resolution (matrix of 192×96, voxel size of $1.9 \times 2.8 \times 7\,\text{mm}^3$) at encoding strengths of 4.0 mm/π.

Phase cycling of the STEAM second RF pulse by 90° allowed storing both the real and imaginary components of the complex position encoded signal along the z-axis during successive acquisitions. The third RF pulse was cycled in synchrony to recall the stored magnetization along the real (X) and imaginary (Y) axes, respectively for signal acquisition. Therefore, the first acquisition samples the real (Re) part of the complex signal, which is the stimulated echo (STE) M plus its complex conjugate M^* (i.e., the stimulated anti-echo, STAE) according to

$$\text{Re}\{M\} = \frac{M + M^*}{2}. \tag{1}$$

The second acquisition samples the imaginary (iIm) part of the complex signal, which is stimulated echo minus the anti-echo according to

$$\text{iIm}\{M\} = \text{i}\frac{M - M^*}{2\text{i}}. \tag{2}$$

The complex stimulated echo signal M is reconstructed by summing the two acquisitions according to

$$M = \text{Re}\{M\} + \text{iIm}\{M\} = |M|\text{e}^{\text{i}\varphi}. \tag{3}$$

Phase image reconstruction to extract the phase φ of the complex signal and strain processing was performed with software written in IDL (Research Systems, Boulder, CO).

3. Results

Fig. 1 shows magnitude phantom images (top row) and their corresponding k-space matrices (bottom row) acquired with a meta-DENSE readout [4] at 4.0 mm/π. The left column shows data acquired with no inversion recovery to suppress the T_1-recovering signal and no RF

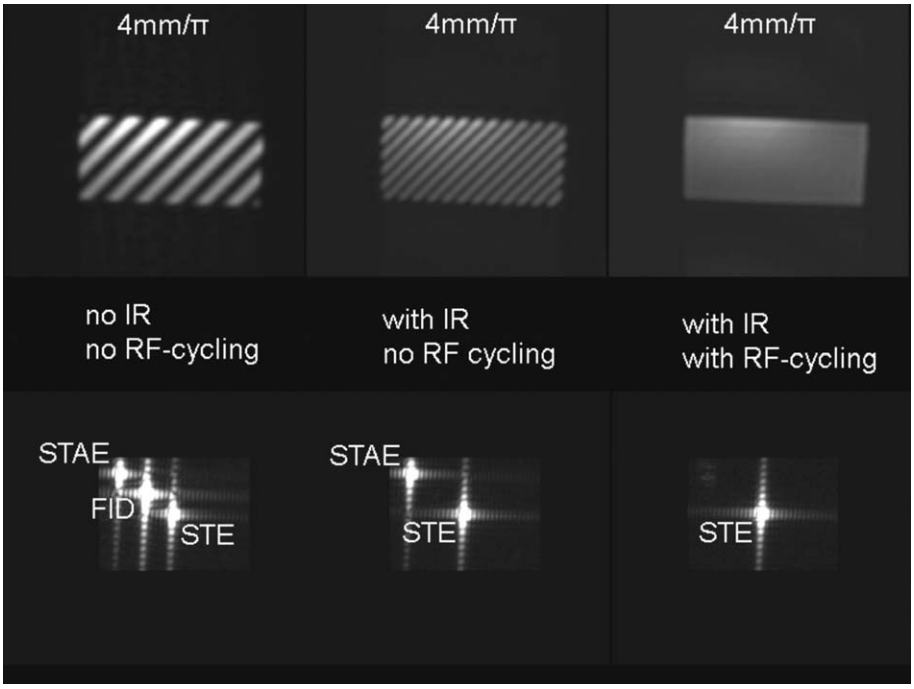

Fig. 1. Suppression of the FID and the STAE reduces tagging artifacts in the image: phantom magnitude images (top row) and corresponding k-space matrices (bottom row) acquired with meta-DENSE at 4.0 mm/π. Compared to the case where no inversion recovery and no RF cycling are used (left column), the inversion recovery addition to meta-DENSE (middle column) results in suppression of the T_1-recovering magnetization (FID) as previously described [4]. The further addition of RF phase cycling for sampling the entire complex STEAM signal (right column) also suppresses the anti-echo, which results in marked suppression of the tag-like artifacts.

phase cycling to suppress the anti-echo. Note the presence of a severe tagging artifact in the image (top left) as a result of the interaction of the three k-space signal components (bottom left). When inversion recovery is applied as described previously [4] but without RF phase cycling, the tagging pattern doubles in frequency (top middle) because the remaining two interacting k-space signal components are spaced twice as far (bottom middle) [8]. When inversion recovery suppression of the T_1-recovering signal is applied along with RF phase cycling scheme to suppress the anti-echo then the tag-like artifacts are suppressed (top right) because the k-space signal sampled contains one spectral component alone (bottom right).

Short axis human magnitude images of the heart acquired with meta-DENSE are shown in Fig. 2 at $2.8 \times 2.8\,mm^2$ pixel size. Fig. 2A shows images without inversion recovery and without RF phase cycling: in this case no tagging artifacts are observed due to the strong encoding gradient moment ($1.2\,mm/\pi$). Fig. 2B has lower encoding gradient moment ($2.0\,mm/\pi$) with inversion recovery applied. Note that the inversion-based suppression does not work in adipose tissue, where the T_1 is different from that of myocardium. Also, note that signal losses in the myocardium are less when compared to Fig. 2A. Fig. 2C shows that reduced gradient encoding moments ($4.0\,mm/\pi$) result in no substantial signal loss in the left ventricle. However, tagging artifacts are now visible. Fig. 2D shows the addition of RF phase cycling at the low encoding gradient moment ($4.0\,mm/\pi$); note the absence of intravoxel dephasing and tagging artifacts in the left ventricle.

Strain maps and their corresponding magnitude images at higher spatial resolution ($1.9 \times 2.8\,mm^2$ pixel size) are shown in Fig. 3, with (top row) and without (bottom row) RF phase cycling. The color scale is from −10 to +20% myocardial strain. All data were acquired with suppression of the T_1-recovering signal at $4.0\,mm/\pi$. The circumferential shortening (CS) and radial thickening (RT) maps are plagued by severe artifacts when RF phase cycling is not applied (bottom row). Note how the tagging artifacts in the magnitude images translate to distorted strain maps. These artifacts are suppressed with the RF phase cycling (top row).

4. Discussion

Phantom and human results with a two acquisition RF phase cycled modified meta-DENSE sequence are shown. The real and imaginary parts of the position encoded signal are combined to yield a complex STEAM signal, which is devoid of the anti-echo and therefore lower encoding strengths than those required with conventional meta-DENSE for a particular pixel size can be used resulting in reduced intravoxel dephasing. In this case, a low gradient encoding strength (which results in $4.0\,mm/\pi$ phase encoding) was demonstrated in-vivo for pixel sizes of 2.8×2.8 and $1.9 \times 2.8\,mm^2$. Fig. 1 shows the evolution of low encoding strength DENSE along the three columns, where the original acquisition (left column) results in tagging artifacts due to the T_1 recovering signal and the STAE [2,3]; the improved DENSE acquisition (center column) with inversion recovery to suppress the longitudinally recovering signal [4]; and last the herein described RF-cycled DENSE with inversion recovery for suppressing also the STAE and removing the tagging-like artifacts.

The application of lower gradient encoding strengths with DENSE can be advantageous in two ways. When collecting phase contrast displacement images, intravoxel dephasing can be the cause of significant signal loss as has been described both by Wedeen et al. [11] and our group [4]. Reducing the gradient encoding moments during the position encoding part of the STEAM experiment alleviates this problem (Fig. 2). Alternatively,

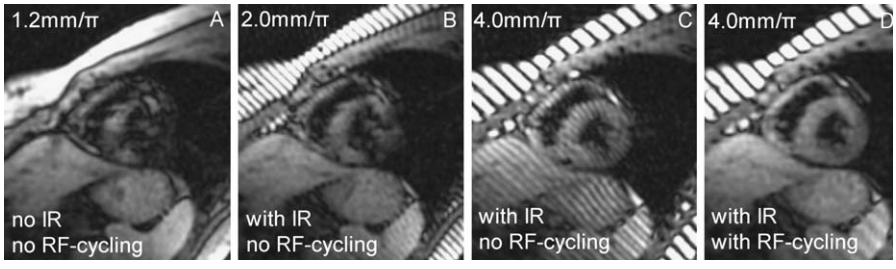

Fig. 2. Trade-offs between signal losses due to intravoxel dephasing and tagging artifacts. (A) The encoding gradient moment has to be strong ($1.2\,mm/\pi$) when no inversion recovery and no RF-cycling is used in order to avoid tagging artifacts. However, intravoxel dephasing due to myocardial deformation results in severe signal loss. Note that no such losses are observed in the liver, which deforms minimally. (B) The addition of inversion recovery to suppress the T_1-recovering signal allows the encoding gradient moment to be lower ($2.0\,mm/\pi$). Intravoxel dephasing signal loss is less but still not acceptable for this healthy volunteer. Note that adipose tissue still is plagued by tagging artifacts due to its short T_1. (C) Further lowering of the encoding gradient moment ($4.0\,mm/\pi$) results in significant improvement in terms of reduced signal loss in the myocardium due to intravoxel dephasing. However, the tagging artifacts in the heart are now severe because the low encoding gradient moment does not push the STAE out of the acquisition window. (D) The combination of inversion recovery, RF phase cycling, and low encoding gradient moments ($4.0\,mm/\pi$) results in markedly reduced tagging artifacts in the myocardium and less intravoxel related signal loss. All images are myocardial short axis human magnitude images at $2.8 \times 2.8\,mm^2$ in-plane resolution, which corresponds to parameters currently used for research patient scans.

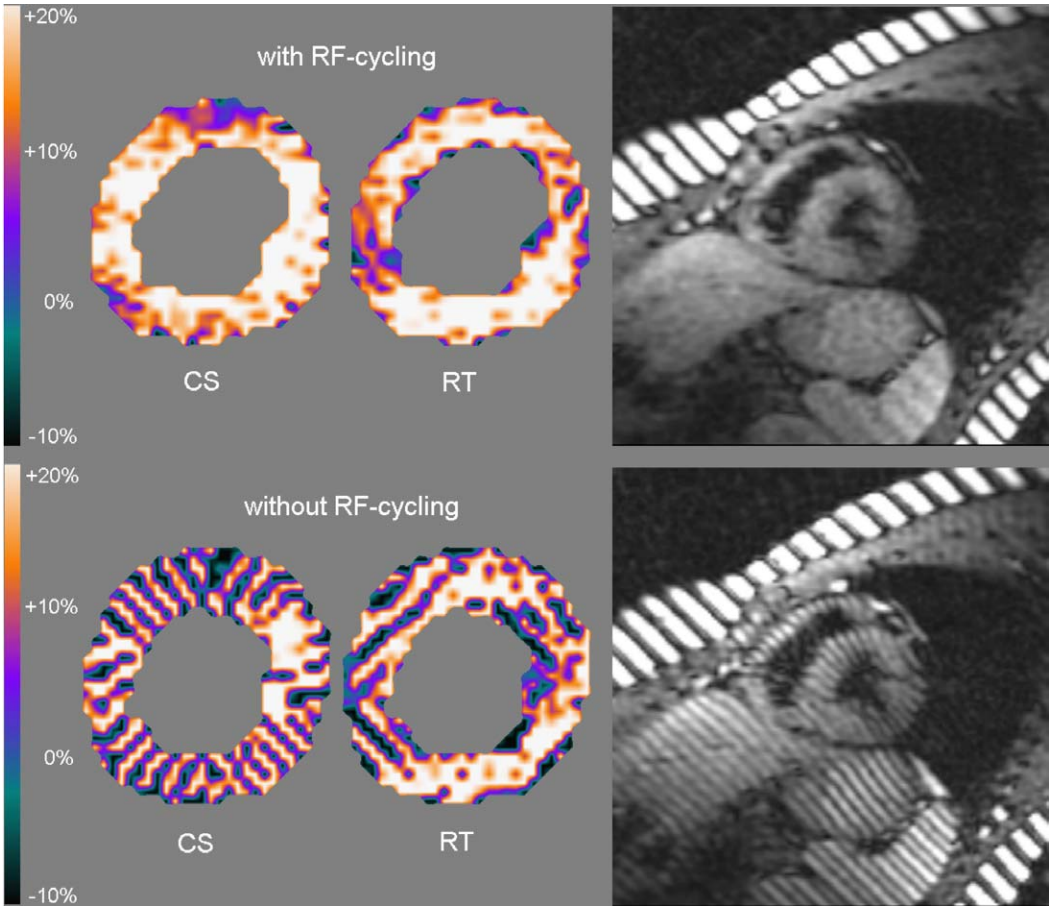

Fig. 3. The application of RF-cycling (top row) suppresses the tagging artifacts in the magnitude image and therefore results in reduced artifacts in the strain maps. When RF-cycling is not present (bottom row), the tagging artifacts seen in the magnitude image result in distorted circumferential shortening and radial thickening maps. Note that data from both X and Y encoded DENSE acquisitions were combined to yield the strain maps; thus resulting in the intricate strain artifacts seen. The color scale is from −10 to +20 percent strain. These higher spatial resolution myocardial short axis human meta-DENSE magnitude images were acquired at $1.9 \times 2.8\,\text{mm}^2$ in-plane resolution and $4\,\text{mm}/\pi$ encoding strength.

for a given such position encoding gradient moment, a larger k-space area can be sampled yielding a smaller pixel size (Fig. 3). The improvement in image quality obtained by both suppressing the T_1 recovering signal [4] and suppressing the anti-echo via RF phase cycling scheme yields strain maps with markedly reduced artifacts (Fig. 3).

References

[1] J. Frahm, W. Hanicke, H. Bruhn, M.L. Gyngell, K.D. Merboldt, High-speed STEAM MRI of the human heart, Magn. Reson. Med. 22 (1) (1991) 133–142.
[2] A.H. Aletras, R.S. Balaban, H. Wen, High-resolution strain analysis of the human heart with fast-DENSE, J. Magn. Reson. 140 (1) (1999) 41–57.
[3] A.H. Aletras, S. Ding, R.S. Balaban, H. Wen, DENSE: displacement encoding with stimulated echoes in cardiac functional MRI, J. Magn. Reson. 137 (1) (1999) 247–252.
[4] A.H. Aletras, H. Wen, Mixed echo train acquisition displacement encoding with stimulated echoes: an optimized DENSE method for in vivo functional imaging of the human heart, Magn. Reson. Med. 46 (3) (2001) 523–534.
[5] D. Kim, W.D. Gilson, C.M. Kramer, F.H. Epstein, Myocardial tissue tracking with two-dimensional cine displacement-encoded MR imaging: development and initial evaluation, Radiology 230 (3) (2004) 862–871.
[6] S.E. Fischer, G.C. McKinnon, S.E. Maier, P. Boesiger, Improved myocardial tagging contrast, Magn. Reson. Med. 30 (2) (1993) 191–200.
[7] S. Ryf, M.A. Spiegel, M. Gerber, P. Boesiger, Myocardial tagging with 3D-CSPAMM, J. Magn. Reson. Imaging 16 (3) (2002) 320–325.
[8] A.H. Aletras, R.Z. Freidlin, G. Navon, A.E. Arai, AIR-SPAMM: alternative inversion recovery spatial modulation of magnetization for myocardial tagging, J. Magn. Reson. 166 (2) (2004) 236–245.
[9] J. Frahm, H. Bruhn, W. Hanicke, K.D. Merboldt, K. Mursch, E. Markakis, Localized proton NMR spectroscopy of brain tumors using short-echo time STEAM sequences, J. Comput. Assist. Tomogr. 15 (6) (1991) 915–922.
[10] J.M. Zhu, I.C. Smith, Stimulated anti-echo selection in spatially localized NMR spectroscopy, J. Magn. Reson. 136 (1) (1999) 1–5.
[11] V.J. Wedeen, R.M. Weisskoff, B.P. Poncelet, MRI signal void due to in-plane motion is all-or-none, Magn. Reson. Med. 32 (1) (1994) 116–120.
[12] F.H. Epstein, W.D. Gilson, Displacement-encoded MRI of the heart using cosine and sine modulation to eliminate artifact generating echoes, Proc. Int. Soc. Magn. Reson Med. 11 (2003) 1566.